

Testing a modified ASKAP Mark II phased array feed on the 64 m Parkes radio telescope

A. P. Chippendale¹ R. J. Beresford¹ X. Deng^{1,2} M. Leach¹
 J. E. Reynolds¹ M. Kramer² T. Tzioumis¹

Abstract — We present the first installation and characterization of a phased array feed (PAF) on the 64 m Parkes radio telescope. The combined system operates best between 0.8 GHz and 1.74 GHz where the beamformed noise temperature is between 45 K and 60 K, the aperture efficiency ranges from 70% to 80%, and the effective field of view is 1.4 deg² at 1310 MHz. After a 6-month trial observing program at Parkes, the PAF will be installed on the 100 m antenna at Effelsberg. This is the first time a PAF has been installed on a large single-antenna radio telescope and made available to astronomers.



Figure 1: Lifting the Mk. II ASKAP PAF, modified for MPIfR, to the focus of the Parkes 64 m radio telescope (credit: J. Sarkissian).

1 INTRODUCTION

Installing a phased array feed (PAF) at the focus of a concentrator, together with digital beamforming, enhances the antenna’s field of view, survey speed, and operational flexibility. This is achieved by forming and processing beams covering many adjacent directions on the sky at the same time.

The Max Planck Institute for Radio Astronomy (MPIfR) is collaborating with CSIRO to deploy a PAF on the Parkes 64 m radio telescope and later on the Effelsberg 100 m telescope. MPIfR and CSIRO will initially use the PAF to look for fast radio bursts (FRBs). These are unexplained radio emissions that last only of order milliseconds but appear to come from the distant universe [1]. The PAF monitors more of the sky at any instant and so increases the chances of discovery and localisation.

CSIRO designed the PAF for the Australian SKA Pathfinder telescope (ASKAP) [2] to demonstrate fast astronomical surveys with a wide field of view for the Square Kilometre Array (SKA) over 0.7 GHz to 1.8 GHz. The SKA is an international project to build the world’s largest radio telescope, with one square kilometre of collecting area.

The ASKAP PAF was designed for the remote Australian SKA site at the Murchison Radio-astronomy Observatory (MRO) within a legislatively protected radio-quiet zone [3]. To operate at Parkes and Effelsberg, the PAF was fitted with narrower sampling filters that accept the 1.2–1.75 GHz band and reject interference from mobile phone and

digital television services at lower frequencies that are far more prevalent at Parkes and Effelsberg.

2 THE MPIfR PAF

The MPIfR PAF is a modified Mk. II ASKAP PAF [4] based on a connected-element “chequerboard” array [5] that is dual-polarized, low-profile, and inherently wide-band. Figure 1 shows the MPIfR PAF being lifted to the focus of the Parkes 64 m radio telescope on 10 February 2016.

To operate an ASKAP PAF in the populous surrounds of Parkes and Effelsberg required modified band preselection to withstand significant terrestrial radio-frequency interference (RFI). The ASKAP and MPIfR filter definitions are compared in Table 1. Reduced MPIfR bandpasses in bands 2 and 3 keep the signal chain linear by rejecting broadband telecom in 694–820 MHz, 850–960 MHz and 1805–1880 MHz, and aeronautical ADS-B/DME at 960–1164 MHz.

The Mk. II PAF system has band-select filters at both ends of all 188 radio frequency over fibre

Band	ASKAP (MHz)	MPIfR (MHz)
1	700–1200	700–1200
2	840–1440	1200–1480
3	1400–1800	1340–1740
4	600–700	600–700

Table 1: ASKAP and MPIfR PAF filters.

¹CSIRO Astronomy and Space Science, PO Box 76, Epping 1710, Australia, e-mail: Aaron.Chippendale@csiro.au.

²Max-Planck-Institut für Radioastronomie (MPIfR), Auf dem Hügel 69, D-53121 Bonn, Germany.

(RFoF) links between the PAF and the digital receiver. In the MPIfR PAF system, only the band-select filters in the PAF have been modified. The filters in the digital receivers are ASKAP units.

The MPIfR PAF requires 60 dB of RF gain to achieve lower than 2 K back-end contribution to system noise and position the drive level to the 12-bit analog-to-digital converter (ADC) inputs at 40 quantisation levels. The 1 dB compression point referred to the array element feed lines is typically better than -60 dBm with 25 dB dynamic headroom to cope with unwanted RFI signals, the main limitation coming from the spurious free dynamic range of the RFoF subsystem, which is $110 \text{ dBHz}^{-2/3}$.

Figures 5–7 show statistics of the 1 MHz resolution spectrum of a single port near the centre of the MPIfR PAF. These measurements were taken with the PAF installed on the Parkes 64 m antenna while it was stowed and pointing near the zenith.

Rejection of RFI by the modified filters in bands 2 and 3 allows the MPIfR PAF to work at Parkes with the same attenuator settings and ADC input levels used for ASKAP at the radio-quiet MRO. In band 1, the MPIfR PAF RF signals require at least 10 dB more attenuation than at the MRO.

3 INSTALLATION AT PARKES

The PAF was installed at the focus of the Parkes 64 m antenna which is a paraboloidal reflector with a focal ratio F/D of 0.41. The phase centre of the PAF, the antenna-side surface of the PAF ground-plane, was positioned to be 24.9 ± 5 mm above the optical focus of the 64 m reflector when the telescope is tipped to 45° elevation. The PAF was installed so that, if the dish were hypothetically tipped to the horizon, the principal polarisation planes of the PAF would be 7.5° clockwise from both the vertical and the horizontal as viewed from the reflector’s vertex looking towards the PAF.

To aid calibration we have installed a radiator at the vertex of the Parkes reflector to transmit broadband noise into the PAF. This is a log-periodic dipole array antenna (Aaronia HyperLOG 7025) with linear polarisation that can be manually rotated, but is nominally left at 45° to the polarisation planes of the PAF elements. PAF port gains may be estimated via correlation of the the PAF RF signals with a direct copy of the radiated calibration noise [6]. Additional fibre was placed in the link carrying the reference copy of the calibration noise so it reaches the digital receiver with the same delay as the noise that is radiated into the PAF.

Initial measurements suggest that calibration via the vertex source will be more complicated on the Parkes 64 m than the promising first attempts on

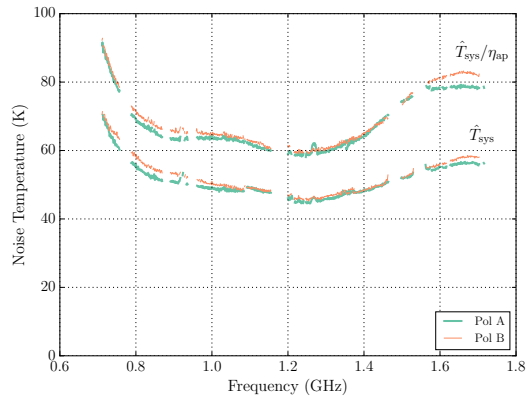


Figure 2: Noise temperature of the MPIfR PAF on the Parkes 64 m antenna. Boresight maxSNR beam.

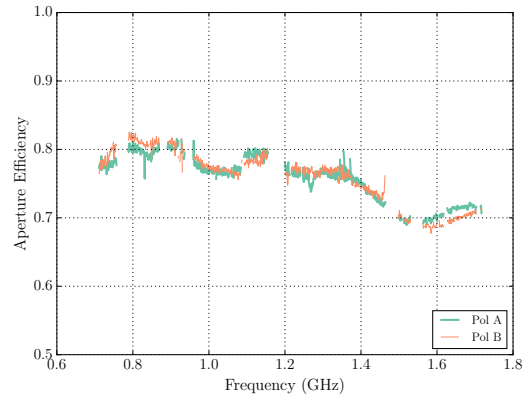


Figure 3: Aperture efficiency η_{ap} of the MPIfR PAF on the Parkes 64 m antenna. Boresight maxSNR beam.

an ASKAP 12 m antenna in [6]. This is due to multipath interference caused by the reflection of the calibration noise from the large floor of the focus cabin at Parkes and then the concentration of this reflection back into the PAF by the paraboloidal reflector. Moving the calibration source away from the vertex may mitigate this effect.

4 PERFORMANCE MEASUREMENTS

Figure 2 shows noise temperatures measured for a boresight beam with maximum signal-to-noise ratio (maxSNR) weights calculated as in [7]. The lower curve is the beam equivalent system noise temperature \hat{T}_{sys} referred to the sky. This is measured via a Y-factor measurement on microwave absorber at ambient temperature, temporarily inserted in front of the PAF while it was at the focus of the Parkes 64 m antenna. The upper curve is the system-temperature-over-efficiency $\hat{T}_{\text{sys}}/\hat{\eta}_{\text{ap}}$ measured via a Y-factor measurement on the radio

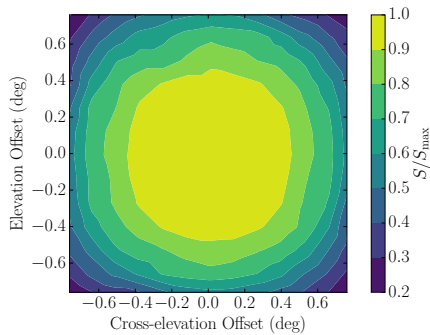


Figure 4: Relative Stokes-I sensitivity S/S_{\max} of the MPIfR PAF on the Parkes 64 m antenna at 1310 MHz.

source Virgo A with known spectral-flux density [8]. We used Vir A both to calculate the beam weights and as the flux standard. Beamforming and flux calibration were performed as per [7] and the hot-load Y-factor measurements follow [9] but use the same beam weights and unobstructed sky reference measurements as the Vir A Y-factor measurements.

Figure 3 shows an estimate of the aperture efficiency η_{ap} formed by dividing \hat{T}_{sys} by $\hat{T}_{\text{sys}}/\eta_{\text{ap}}$. All sky measurements were made between elevations of 35.4° and 48.0° . Gaps in frequency coverage are due to the removal of data affected by RFI.

Figure 4 shows the envelope of Stokes-I sensitivity S over the field-of-view normalised by the peak sensitivity S_{\max} . This was calculated by repeating the Y-factor measurement on Vir A over a 13×13 grid of antenna offset pointings with 0.13° pitch and using maxSNR weights calculated independently for each pointing. Integrating $(S/S_{\max})^2$ over the field of view results in an effective field of view of 1.4 deg^2 following the definition of [10].

5 CONCLUSION

We have demonstrated that the MPIfR PAF can achieve a noise temperature as low as 45 K and an aperture efficiency of 70% to 80% on the Parkes 64 m antenna. It is encouraging that the modified filters for bands 2 and 3 reject sufficient RFI at Parkes for the radio-over-fibre architecture to work at the same operating power levels intended for the radio-quiet MRO. Good sensitivity was also demonstrated in band 1, but we are yet to learn what fraction of time RFI conditions might exceed the limited headroom in band 1.

Acknowledgments

The Max-Planck Institute for Radio Astronomy financed the PAF discussed in this paper and its

modification for a less radio-quiet site. Installation, operation and testing at Parkes was supported by A. Dunning, Dr. D. Hayman, S. Hegarty, J. Kanapathippillai, M. Marquarding, B. Preisig, Dr. W. Raja, T. Ruckley, M. Smith, and Dr. G. Wieching. The Parkes radio telescope is part of the Australia Telescope National Facility which is funded by the Australian Government for operation as a National Facility managed by CSIRO.

References

- [1] Thornton, D., Stappers, B., Bailes, M., et al. 2013, *Science*, 341, 53
- [2] D. R. DeBoer et al. Australian SKA Pathfinder: A high-dynamic range wide-field of view survey telescope. *Proc. IEEE*, 97(8):1507–1521, Aug. 2009.
- [3] C. Wilson, M. Storey, and T. Tzioumis. Measures for control of EMI and RFI at the Murchison Radioastronomy Observatory, Australia. In *Electromagnetic Compatibility (APEMC), 2013 Asia-Pacific Symposium on*, pp. 1–4, May. 2013.
- [4] G. Hampson et al. ASKAP PAF ADE – advancing an L-band PAF design towards SKA. In *Electromagnetics in Advanced Applications (ICEAA), 2012 International Conference on*, pp. 807–809, Sept. 2012.
- [5] S. G. Hay and J. D. O’Sullivan. Analysis of common-mode effects in a dual-polarized planar connected-array antenna. *Radio Sci.*, 43(6), Dec. 2008.
- [6] A. P. Chippendale et al. Recent developments in measuring signal and noise in phased array feeds at CSIRO. *Antennas and Propagation (EuCAP), 2016 European Conference on*, Apr. 2016.
- [7] A. P. Chippendale et al. Measured sensitivity of the first Mark II phased array feed on an ASKAP antenna. In *Electromagnetics in Advanced Applications (ICEAA), 2015 International Conference on*, Nov. 2015.
- [8] M. Ott et al. An updated list of radio flux density calibrators. *Astronomy and Astrophysics*, 284:331–339, Apr. 1994.
- [9] A. P. Chippendale et al. Measured aperture-array noise temperature of the Mark II phased array feed for ASKAP. In *Antennas and Propagation (ISAP), 2015 International Symposium on*, Sept. 2015.
- [10] J. D. Bunton and S. G. Hay. Achievable field of view of chequerboard phased array feed. In *Electromagnetics in Advanced Applications (ICEAA), 2010 International Conference on*, pp. 728–730, Sept. 2010.

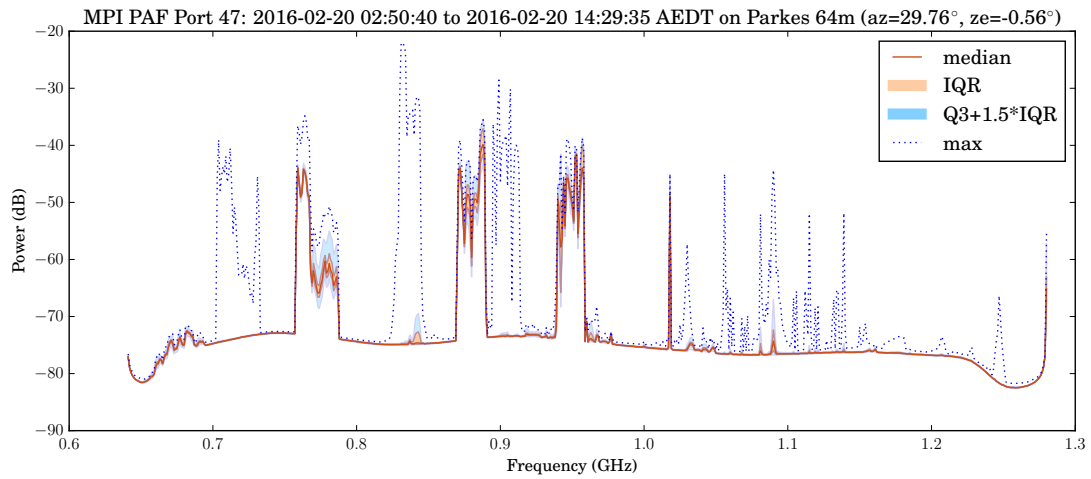


Figure 5: Band 1 spectrum statistics at Parkes with 1 MHz resolution.

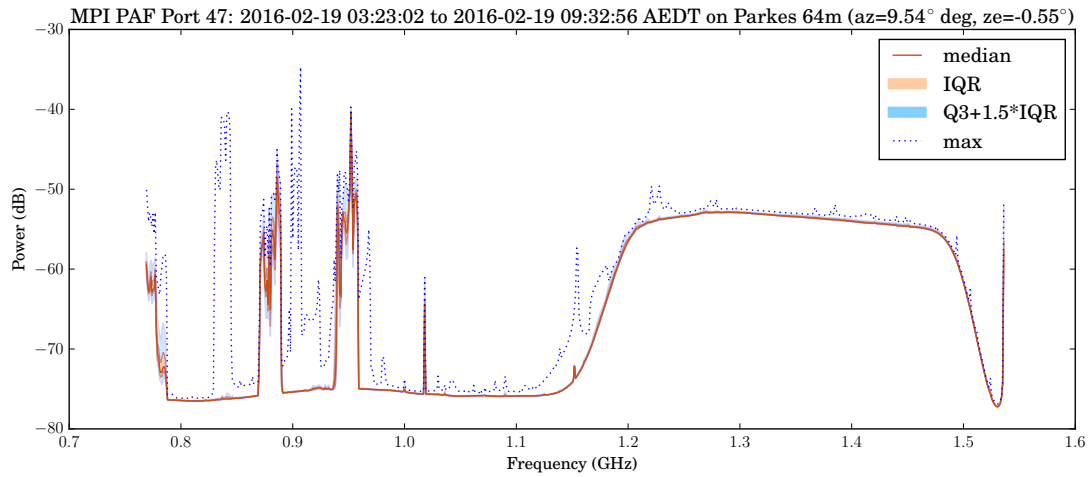


Figure 6: Band 2 spectrum statistics at Parkes with 1 MHz resolution.

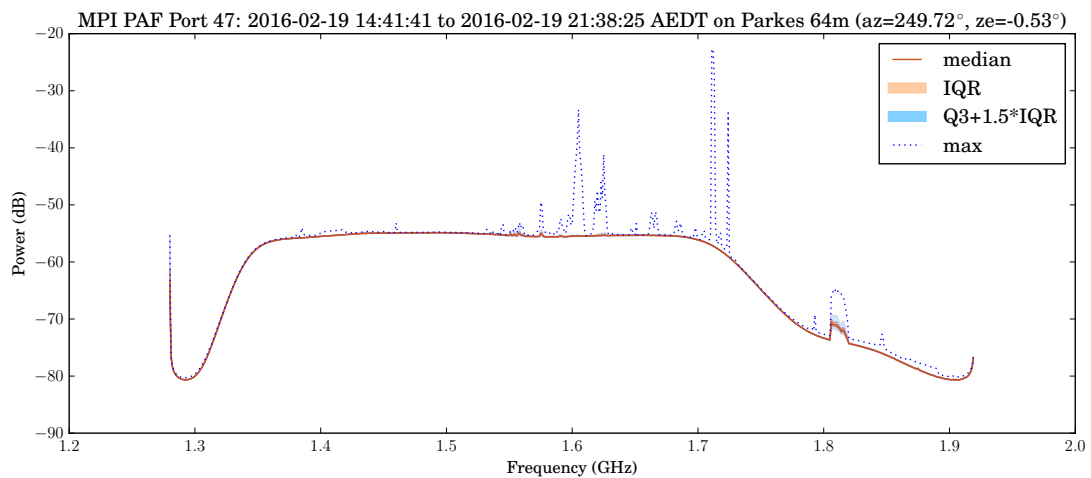


Figure 7: Band 3 spectrum statistics at Parkes with 1 MHz resolution.